



Mesoporous Germanium Formation by Electrochemical Etching

E. Garralaga Rojas,^{a,z} H. Plagwitz,^a B. Terheiden,^a J. Hensen,^a C. Baur,^b
G. La Roche,^c G. F. X. Strobl,^c and R. Brendel^a

^aInstitut für Solarenergieforschung Hameln, D-31860 Emmerthal, Germany

^bEuropean Space Agency/European Space Research and Technology Centre, NL-2200 AG Noordwijk, The Netherlands

^cAZUR SPACE Solar Power GmbH, D-74072 Heilbronn, Germany

Uniform thick mesoporous germanium layers are reproducibly formed on 4 in. p-type Ge wafers by electrochemical etching in highly concentrated HF electrolytes. Pore formation by anodic etching in germanium leads to a constant dissolution of the porous layer. The growth rate of the porous Ge layer is therefore given by the difference between the etch rate at the porous layer/substrate wafer interface and the dissolution rate at the electrolyte/porous layer interface. The growth rate lies in the range of 0.071–2.7 nm/min for etching current densities of 0.1–80 mA/cm², while both the etch rate and the dissolution rate lie in the range of several micrometers per minute. We define the substrate usage as the ratio of the growth rate and the etch rate. This substrate usage determines the growth efficiency of the porous layer and lies in the range of 0.2–2%. Thus, the substrate wafer is thinned substantially during anodic porous layer formation. Constantly alternating from an anodic to a cathodic bias prevents the thinning of the substrate. The dissolution rate decreases, and the usage increases up to 98%.
© 2009 The Electrochemical Society. [DOI: 10.1149/1.3147271] All rights reserved.

Manuscript submitted March 26, 2009; revised manuscript received May 5, 2009. Published June 10, 2009.

The reduction in the weight of multijunction III-V semiconductor solar cells is an important budget issue for space applications. Multijunction space solar cells are epitaxially formed on a Ge substrate wafer. The substrate material determines the lattice constant of the stack, provides mechanical stability during the cell process, and serves as a bottom cell.¹ For reasons of mechanical stability during the cell process, this substrate wafer is typically more than 100 μm thick, whereas a few micrometer thickness would be sufficient for the bottom cell to match the photogenerated currents in the top and middle cells. As a consequence, these unnecessarily heavy substrate wafers reduce the available payload for satellite missions.

There are several techniques that permit the production of lightweight highly efficient space solar cells. The Ge or GaAs substrates are commonly removed by chemical wet etching,² which reduces weight but has the disadvantage that the substrate wafer is lost. Separating the electrically active solar cells from their substrates by a lift-off process could save the substrate.

For the fabrication of monocrystalline silicon solar cells, lift-off processes based on the epitaxial growth of the absorber layer onto a porous-etched substrate already exist. Brendel³ demonstrated the so-called porous silicon process for the production of monocrystalline thin-film Si solar cells. This method uses a double layer of mesoporous Si formed by electrochemical etching: A mesoporous layer with low porosity at the surface of the substrate is used as a seed layer for the Si epitaxy, while a buried highly porous layer is used as a pre-determined breaking point.

Only a few publications on porous germanium (PGe) were published.^{4–17} Flaman et al.¹¹ studied porous Ge formation in HF-based electrolytes and the possibility of using PGe for a lift-off process. However, the authors apparently did not find suitable etching conditions for lift-off. Strong nonuniform macropores were achieved. Thus, the formation of homogeneous electrochemically etched mesoporous Ge was not yet reported.

In this paper, we show a procedure to form uniform mesoporous Ge layers by electrochemical etching using HF-based electrolytes. This process is demonstrated on 4 in. Ge.

Experimental

The Ge wafers used in this investigation were monocrystalline, 4 in. in diameter, and one-side polished. They were (150 ± 10) μm thick. Their orientation was {100}, and the specific resistivity was (25 ± 15) mΩ cm.

A double-container etching cell was used to anodize the wafers. Aqueous HF with a concentration varying in the range of 2–50% served as an electrolyte. The cathodic electrical contact from the electrolyte to the Ge wafer was obtained due to its high dopant concentration. The potentiostat Elypor 3 from the company ET&TE Etch and Technology GmbH allowed various etching profiles, i.e., current or voltage vs time profiles to be programmed. The etching current density was set to a fixed value, and the etching potential was automatically adjusted to obtain the desired etching current density (Fig. 1).

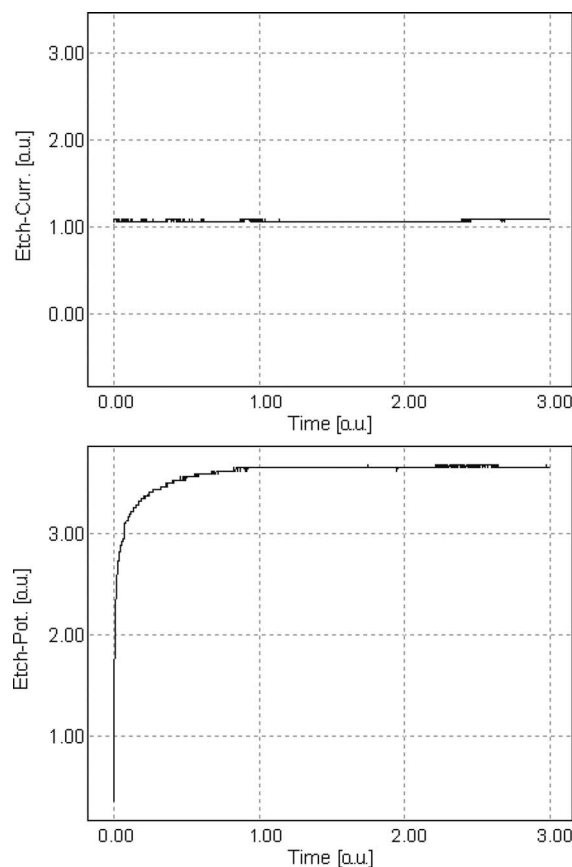


Figure 1. Anodic etching profile in galvanostatic mode.

^z E-mail: e.garralaga@isfh.de



Figure 2. (Color online) Electrochemically etched (100) p-type Ge wafer, 50 wt % HF, $j = 1 \text{ mA/cm}^2$, and $t = 3 \text{ h}$. Note that the dashed line represents the region at which the porous layer thickness has a maximum variation of 30 nm.

After etching, the samples were rinsed in deionized water and dried under a N_2 stream. We inspected the morphology and thicknesses of the porous layers in a high resolution Hitachi S-4800 scanning electron microscope (SEM).

Results for Anodic Etching

Figure 2 shows the plane view of a 4 in. Ge wafer after etching and subsequent rinsing and drying. The inner part of the wafer is homogeneously colored, indicating that the porosity and thickness of the porous layer are also homogeneous. The SEM analysis shows indeed a mean porous layer thickness of 160 nm with a maximum variation in thickness of 30 nm within the dashed line in Fig. 2.

At the rim of the wafer, a stripe of a different color is produced by the sample holder, caused by an inhomogeneous current flow. The colors are Fabry–Perot interference fringes originating from reflections at the air/PGe and PGe/substrate interfaces.

Figure 3 shows the cross-sectional SEM image of a 4 in. Ge wafer. The diameter of the pores lies in the range of 1–46 nm, and the mean diameter of the pores is 15.7 nm. According to the Inter-

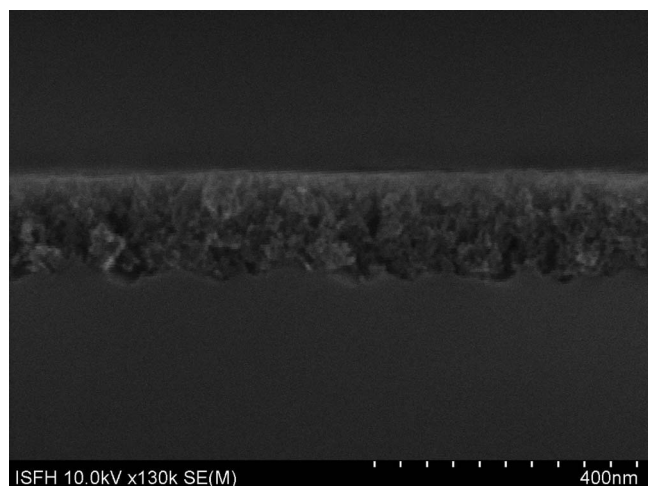


Figure 3. SEM image of the cross section of a PGe layer. (100) p-type Ge, 50 wt % HF, $j = 1 \text{ mA/cm}^2$, and $t = 3 \text{ h}$.

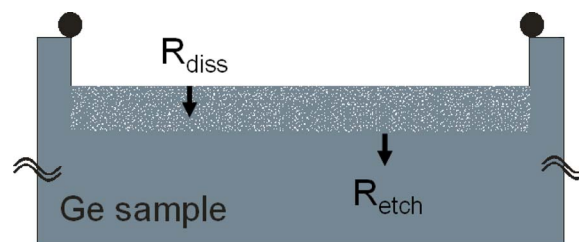


Figure 4. (Color online) Porous Ge etching growth schema.

national Union of Pure and Applied Chemistry,¹⁸ mesopores range from 2 to 50 nm. Our porous Ge layer is thus composed of mesopores. The surface roughness is less than 10 nm, and the roughness at the PGe/substrate interface is less than 20 nm.

Porous Ge formation is accompanied by the constant dissolution of the already porosified surface. Figure 4 introduces two etching rates, R_{etch} and R_{diss} . The porous layer etching rate R_{etch} is the velocity at which the porous layer grows into the sample. The already formed porous layer is continuously dissolved at its upper surface. The porous layer dissolution rate R_{diss} denotes the velocity at which the porous layer dissolves, thus limiting the growth rate of the porous layer. The growth rate of the mesoporous layer, $R_{\text{growth}} = R_{\text{etch}} - R_{\text{diss}}$, gives the difference between the etching rate and the dissolution rate.

We calculate R_{diss} by linearly fitting the remaining thickness of the substrate and the thickness of the porous layer as a function of the etching duration. The slope of the linear fit gives the porous layer dissolution rate. Figure 5 shows the porous layer dissolution rates obtained for 40 wt % HF in water and in ethanol as a function of the etching current density. We obtain dissolution rates of 0.011–1.33 $\mu\text{m}/\text{min}$ depending on the etching current applied and on the solvent used. We find two linear regimes in a semilogarithmic plot of the dissolution rates of the PGe layer shown in Fig. 5, below and above 7.5 mA/cm^2 .

To reduce the dissolution of the PGe layer, very low etching current densities have to be applied. Figure 5 shows that ethanolic electrolytes dissolve the substrate faster than aqueous electrolytes. We relate this effect to the wetting properties of ethanol as it enhances the wettability of the substrate and helps to remove hydrogen bubbles that are produced through the electrochemical etching of

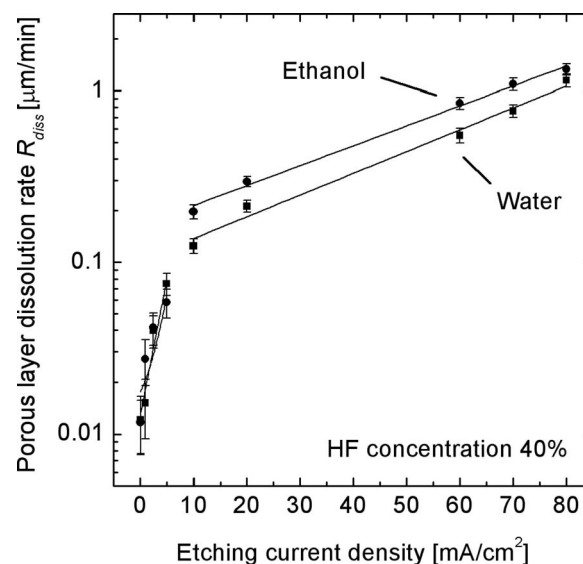


Figure 5. Porous layer dissolution rate vs etching current density.

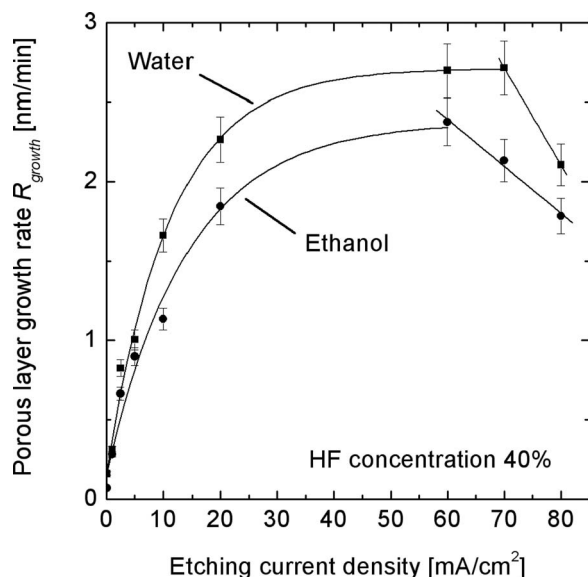


Figure 6. Porous layer growth rate vs etching current density.

Ge. Because H_2 bubbles hinder PGe formation and etching, the use of ethanoic electrolytes allows a faster dissolution of the substrate.

We obtain R_{growth} from the slope of a linear fit to the porous layer thicknesses measured by SEM as a function of the etching duration for both aqueous and ethanoic electrolytes and for several current density values. R_{growth} lies in the range between 0.071 and 2.7 nm/min for etching currents between 0.1 and 80 mA/cm². Figure 6 shows the porous layer growth rate as a function of the etching current density.

Aqueous solutions show higher growth rates R_{growth} than ethanoic solutions. This effect is related to the increased dissolution rate of the porous layer in ethanol. Because R_{growth} is given by the difference between R_{etch} and R_{diss} , the porous layer growth rate is limited by R_{diss} . Ethanoic electrolytes present high dissolution rates R_{diss} ; the fast dissolution of the porous layer therefore limits R_{growth} . High etching current densities above 60 mA/cm² lead to a decrease in R_{growth} for both ethanoic and aqueous electrolytes due to the in-

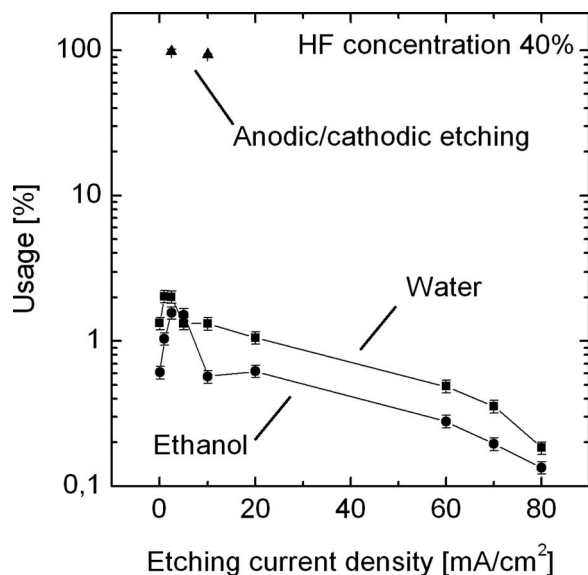


Figure 7. Usage vs etching current density.

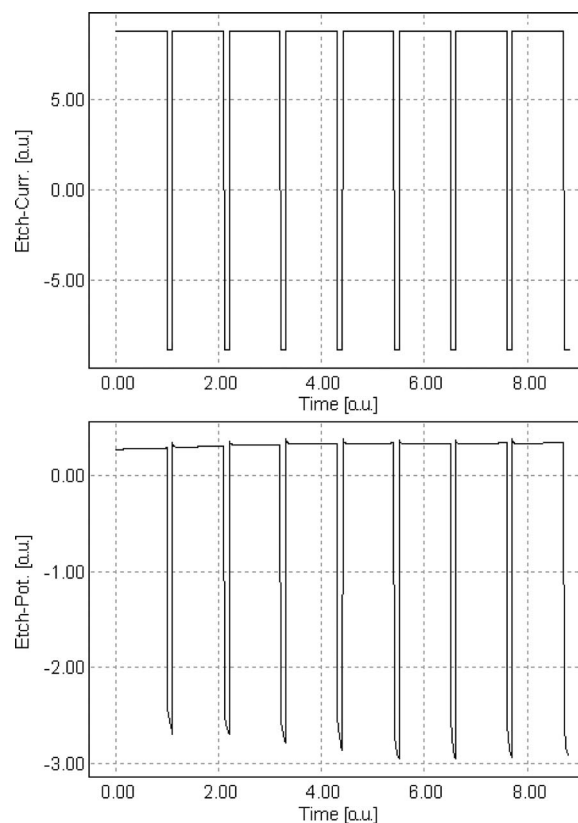


Figure 8. Etching profile in galvanostatic mode.

creasing R_{diss} . Etching current densities higher than 80 mA/cm² do not even allow for porous layer formation as the increased R_{diss} simply leads to the electropolishing of the wafer.

We define the substrate usage

$$U = R_{\text{growth}}/R_{\text{etch}} \quad [1]$$

that quantifies the volume efficiency for transforming a nonporous bulk material into a porous material.

Figure 7 shows the substrate usage of anodic porous Ge formation as a function of the etching current. Because R_{growth} is around 2–3 orders of magnitude smaller than R_{etch} , the usage is very low, in the range of 0.2–2.0%, thus showing a very inefficient porous layer growth. Several micrometers of material are consumed to obtain a porous layer of a few hundreds of nanometers.

Results for Anodic/Cathodic Etching

Hydrogen passivation of the surface reduces substrate thinning. Turner¹⁹ carried out oscillographic investigations of the Ge surface by constantly changing the polarization direction. He found the cathodic reactions to proceed in two steps: First, the Ge oxide at the surface is reduced. Second, hydrogen atoms bond to Ge surface atoms. The surface is thereby passivated, the porous layer stops to grow, and germane (soluble or gas) compounds form at the surface of the cathode.²⁰ The reaction equation is



Choi and Buriak¹² produced PGe by alternating the etching bias. Fang et al.⁹ proposed a mechanism that increases the passivation of the Ge surface by switching the system periodically from an anodic to a cathodic bias. The passivation provided by the cathodic step inhibits the dissolution of the already formed porous layer. However, the duration of the passivation is limited. It depends mainly on the etching current density of the subsequent anodic step and the electrolyte concentration. High etching current densities and electrolyte

concentrations decrease the duration of the passivation effect. Typically, passivation lasts 1–10 min. A cathodic step is necessary afterward to further passivate the surface.

Figure 8 shows the etching current density and etching potential profiles that we apply in this paper in arbitrary units. We pulse the system eight times from the anodic to the cathodic bias by changing the etching current density to passivate the surface.

Due to the increased passivation, R_{diss} decreases substantially, becoming almost zero. The passivation also affects R_{etch} , reducing the rate down to values similar to R_{growth} in the nanometer range. Because both R_{growth} and R_{etch} take similar values, the substrate usage increases substantially. Figure 7 shows that usage values in the range of 93–98% are obtained using this technique. The initial phase of the porous layer growth, also called the nucleation phase, causes substrate thinning until pore growth starts. This phase, common to all materials, usually removes a few micrometers of substrate until homogeneous nucleation is achieved. Higher usage values are therefore hardly possible due to initial substrate etching.

Conclusions

We obtained mesoporous Ge by electrochemical etching. Porous Ge layers have two etching fronts, one at the top, which is responsible for the thinning of the substrate, and one at its bottom, which causes the growth of the mesoporous layer. The dissolution rate of the already formed PGe lies in the range of 0.011–1.33 $\mu\text{m}/\text{min}$ for etching current densities of 0.1–80 mA/cm^2 . The growth rate of the porous layer lies in the range of 0.071–2.7 nm/min . In comparison to aqueous electrolytes, ethanoic solutions do have a higher dissolution rate, thus yielding a thinner sample. We presented a technique that allows porous Ge layer growth and avoids substrate thinning based on alternating between anodic and cathodic biases. The substrate usage drastically increases from values of 0.002–0.02 for anodically etched samples to values of 0.98 for samples using this technique.

Acknowledgment

The authors thank Sebastian Gatz, Andreas Wolf, and Marco Ernst from the ISFH and Professor Helmut Föll and Jürgen

Carstensen from the University of Kiel for fruitful discussions and Bianca Gehring for technical assistance. The financial support of this work by the German Ministry for Economy and Technology under contract no. 50JR0641 is gratefully acknowledged. E.G.R. especially thanks the European Space Agency for the financial support of his work in the framework of the Networking Partnering Initiative (contract no. 20250/06/NL/GLC).

References

1. M. Meusel, W. Bensch, T. Bergunde, R. Kern, V. Khorenko, W. Köstler, G. LaRoche, T. Torunski, W. Zimmermann, G. Strobl, et al., in *Proceedings of the 22nd EUPVSEC*, WIP, Milano, pp. 16–21 (2007).
2. J. F. Geisz, S. Kurtz, M. W. Wanlass, J. S. Ward, A. Duda, D. J. Friedman, J. M. Olson, W. E. McMahon, T. E. Moriarty, and J. T. Kiehl, *Appl. Phys. Lett.*, **91**, 023502 (2007).
3. R. Brendel, in *Proceedings of the 14th EUPVSEC*, WIP, Barcelona, pp. 1354–1357 (1997).
4. S. Langa, M. Christophersen, J. Carstensen, I. M. Tiginyanu, and H. Föll, *Phys. Status Solidi A*, **195**, R4 (2003).
5. S. Langa, J. Carstensen, M. Christophersen, K. Steen, S. Frey, I. M. Tiginyanu, and H. Föll, *J. Electrochem. Soc.*, **152**, C525 (2005).
6. S. Langa, J. Carstensen, I. M. Tiginyanu, and H. Föll, *Phys. Status Solidi C*, **2**, 3237 (2005).
7. H. Föll, J. Carstensen, and S. Frey, *J. Nanomater.*, **2006**, 1 (2006).
8. C. Fang, H. Föll, and J. Carstensen, *Nano Lett.*, **6**, 1578 (2006).
9. C. Fang, H. Föll, and J. Carstensen, *J. Electroanal. Chem.*, **589**, 259 (2006).
10. C. Fang, H. Föll, J. Carstensen, and S. Langa, *Phys. Status Solidi A*, **204**, 1292 (2007).
11. G. Flamand, J. Poortmans, and K. Dessein, *Phys. Status Solidi C*, **2**, 3243 (2005).
12. H. C. Choi and J. Buriak, *Chem. Commun. (Cambridge)*, **2000**, 1669.
13. J. Buriak, *Chem. Rev. (Washington, D.C.)*, **102**, 1271 (2002).
14. J. Shieh, H. L. Chen, T. S. Ko, H. C. Cheng, and T. C. Chu, *Adv. Mater. (Weinheim, Ger.)*, **16**, 1121 (2004).
15. L. K. van Vugt, A. F. van Driel, R. W. Tjerkstra, L. Bechger, W. L. Vos, D. Vanmaekelbergh, and J. J. Kelly, *Chem. Commun. (Cambridge)*, **2002**, 2054.
16. D. Sun, A. Riley, A. Cadby, E. Richman, S. Korlann, and S. Tolbert, *Nature (London)*, **441**, 1126 (2006).
17. G. Armatas and M. Kanatzidis, *Nature (London)*, **441**, 1122 (2006).
18. J. Rouquerol, D. Avnir, C. W. Fairbridge, D. H. Everett, J. M. Haynes, N. Pernicone, J. D. F. Ramsay, K. S. W. Sing, and K. K. Unger, *Pure Appl. Chem.*, **66**, 1739 (1994).
19. D. Turner, *J. Electrochem. Soc.*, **103**, 252 (1956).
20. P. F. Schmidt and C. Church, *J. Electrochem. Soc.*, **108**, 296 (1961).